Research Article

Aleksandra Ciesielska, Wojciech Ciesielski*, Henryk Kołoczek, Damian Kulawik, Joanna Kończyk, Zdzislaw Oszczęda, Piotr Tomasik

Structure and some physicochemical and functional properties of water treated under ammonia with low-temperature low-pressure glow plasma of low frequency

https://doi.org/10.1515/chem-2020-0166
received May 30, 2020; accepted August 19, 2020

Abstract: Deionized, tap and two kinds of commercially available mineralized water, after supplementation with ammonia, were treated with low-pressure, low-temperature glow plasma (GP) of low frequency. Treating hard water with ammonia provided the removal of permanent and temporary water hardness already at room temperature. On such treatment, mineralized water supplemented with ammonia was partly demineralized. Precipitated rhombohedral deposit from hard water did not turn into scale even when maintained in suspension for 3 days at around 90°C. In such manner, the use of other chemicals for prevention from the scale formation and/or for the scale removal is entirely dispensable. The rate and yield of precipitation depended on the concentration of admixed ammonia and the GP treatment time. Ammonia served as a ligand of calcium, magnesium and ferric central atoms of corresponding salts constituting the hardness. Moreover, ammonia constituting the atmosphere of the treatment was arrested inside aqueous clathrates. So, stabilized ammonia solutions could potentially be utilized as an environmental-friendly nitrogen fertilizer. The precipitate could also be utilized for the same purpose.

Keywords: ammonia ligand, aqueous clathtrates, environmentally friendly nitrogen fertilizer, scale prevention

*** Corresponding author: Wojciech Ciesielski,** Institute of Chemistry, Jan Długosz University, Armii Krajowej Ave., 13-15, Częstochowa, Poland, e-mail: w.ciesielski@interia.pl
Aleksandra Ciesielska: Faculty of Chemistry, University of Gdansk, Wita Stwosza St. 63, 80-308, Gdansk, Poland, e-mail: olaciesielska5@gmail.com
Henryk Kołoczek: Institute of Chemistry and Inorganic Technology, Krakow University of Technology, Warszawska Str. 24, 31 155, Krakow, Poland, e-mail: koloczek@indy.chemia.pk.edu.pl
Damian Kulawik: Institute of Chemistry, Jan Długosz University, Armii Krajowej Ave., 13-15, Częstochowa, Poland, e-mail: d.kulawik@ujd.edu.pl
Joanna Kończyk: Institute of Chemistry, Jan Długosz University, Armii Krajowej Ave., 13-15, Częstochowa, Poland, e-mail: j.konczyk@ujd.edu.pl
Zdzislaw Oszczęda: Nantes Nanotechnological Systems, Dolnych Młynów Str. 24, 59 700, Bolesławiec, Poland, e-mail: z.oszczeda@nantes.com
Piotr Tomasik: Nantes Nanotechnological Systems, Dolnych Młynów Str. 24, 59 700, Bolesławiec, Poland, e-mail: rrtomasi@cyf-kr.edu.pl

1 Introduction

From a chemical point of view, water which is commonly used in everyday life cannot be considered pure. Even when either redistilled or thoroughly deionized, it is, in fact, a solution of components of the atmosphere in which these operations were carried out. The gaseous components cannot be fully evacuated from those solutions even under a deep vacuum. Such water, particularly when containing dissolved oxygen, is corrosive which is essential on its technical applications. If not either deionized or distilled, water contains dissolved mineral salts. Sulfates and hydrogen carbonates of calcium, magnesium and iron are responsible for the so-called permanent and temporary water hardness, and the other salts constitute water mineralization. Both kinds of hardness cause a scale deposition in water-heating systems and water-transmitting pipelines. Calcium and magnesium sulfates precipitate and go into scale after reaching the saturation point in a given solution. In contrast to them, magnesium and chiefly calcium bicarbonates precipitate even from their diluted solutions because of the shift in the equilibrium of the reaction

$$Ca(HCO_3)_2 \rightleftarrows CaCO_3 + H_2O + CO_2$$

to the right side. Water-soluble hydrogen carbonate decomposes into water insoluble carbonate, water and CO_2. Calcium carbonate precipitates as rhombohedral aragonite forming a mud which successively turns into developing scale rhombic calcite.

There are several unwanted consequences of the scale formation. The costs of heating water in the scale-

covered heating systems producing hot water and/or steam increase. Perturbed heat transmission can result in local overheating. Gradual closing pipes require more energy for transmitting fluids across them.

In order to manage with scale, two approaches are in use. One prevents the scale formation and the other takes its removal once it forms. The most common methods involve (i) deionization of water with ion exchangers, (ii) blowing CO_2 into water to hinder the decomposition of calcium/magnesium hydrogen carbonate into the corresponding carbonates, (iii) addition of polyphosphates and (iv) treatment of water with static magnetic as well as electric field. Once the precipitate of aragonite is formed, it should be removed prior to its conversion into calcite scale by either blowing with steam or air or by filtration. Moreover, (v) the removal of hardness through an accelerated precipitation of calcium carbonate may be involved. For this purpose, a blend of lime and sodium carbonate is added at 60–80°C. The selected approach depends on the destination of the water after the treatment, parameters of the installation prevented from the scale and, generally, economy of the process [1–5].

In former papers, the ability of low-temperature, low-pressure glow plasma (GP) of low frequency to modulate water macrostructure and, hence, its physical, physicochemical and functional properties was demonstrated. These properties depended, among others, on the time of exposure of the water to GP and the atmosphere under which the GP treatment was performed. Thus far, the effect of the air [6], oxygen-free nitrogen [7], carbon dioxide [8], methane [9] and oxygen [10] upon results of the GP treatment was published. In the course of our studies, we found that the energy of applied GP never broke valence bonds and could not initiate any chemical reaction. Thus, on the treatment of water in the air as well as under pure oxygen, neither hydrogen peroxide nor ozone was formed.

In this paper, results of the GP treatment upon either deionized or tap water under ammonia are presented. The preparation of water with potentially interesting functional properties was the driving force for this study. It has appeared that such treatment of water offered a simple removal of permanent and temporary water hardness. A fine mineral deposit which was formed had no tendency to turn into the scale. In such manner, any involvement of other chemicals appeared dispensable. Resulting water hosting ammonia in aqueous clathrates was practically odorless. Therefore, it could be either comfortably recirculated or potentially utilized as environmentally benign nitrogen fertilizer. For its composition, the precipitates could also be utilized for the same purpose.

2 Materials and methods

2.1 Water characteristics

- Commercially available deionized water contained totally 20.04 mg minerals/L (0.25 mg Ca^{2+}/L, 0.12 mg Mg^{2+}/L, 0.08 mg Na^{+}/L, 18.30 mg $HCO_3^{=}$/L, 1.28 mg $SO_4^{=}$/L, 0.01 mg Cl^{-}/L).
- Tap water: municipal water from the Czestochowa supply system containing totally 672.28 mg minerals/L (193.27 mg Ca^{2+}/L, 46.21 mg Mg^{2+}/L, 23.18 mg Na^{+}/L, 5.27 mg K^{+}/L, 351.90 mg $HCO_3^{=}$/L, 51.20 mg $SO_4^{=}$/L, 6.52 mg Cl^{-}/L and 40 µg Fe/L).
- Highly mineralized water: Commercially available water "Kryniczanka" highly saturated with CO_2 containing totally 2246.1 mg minerals/L (368.92 mg Ca^{2+}/L, 73.209 mg Mg^{2+}/L, 54.71 mg Na^{+}/L, 5.27 mg K^{+}/L, 1721.9 mg $HCO_3^{=}$/L, 40.50 mg $SO_4^{=}$/L, 7.8 mg Cl^{-}/L and 0.4 mg F^{-}/L).
- Weakly mineralized water: Commercially available nonsaturated with CO_2 water "Kropla Beskidu" containing totally 322.27 mg minerals/L (44.9 mg Ca^{2+}/L, 17.01 mg Mg^{2+}/L, 11.10 mg Na^{+}/L, 1.0 mg K^{+}/L, 186.7 mg $HCO_3^{=}$/L, 43.62 mg $SO_4^{=}$/L and 3.19 mg Cl^{-}/L).

2.2 Methods

2.2.1 Water treatment with GP

Either deionized, tap, high- or low-mineralized water (100 mL) was blended either with (i) saturated at room temperature aqueous ammonia puriss., anhydrous, ≥99.95% (Sigma-Aldrich, Warsaw, Poland) (1, 2.5, 5, 7.5 or 10 mL) or with (ii) aqueous 0.01 M solution of sodium hydroxide anhydrous, free-flowing pellets, ≥97% (Sigma-Aldrich) (1, 5 or 10 mL) and placed within 250 mL polyethylene bottles. The bottles were transferred into the chamber of the reactor [11,12] and exposed to plasma for either 1, 5, 15, 30, 60 or 120 min. Plasma of 38°C was generated at 5×10^{-3} mbar, 600 V, 50 mA and 280 GHz frequency. The corresponding nontreated water and the corresponding nontreated aqueous hydroxide

solutions served as primary and secondary controls, respectively.

2.2.2 pH measurements

pH values were taken at ambient temperature (~20°C) with the Metrohm 827 lab pH meter Metrohm Polska Sp. z o.o. (Opacz-Kolonia, Poland). The measurements were run in triplicates.

2.2.3 Conductivity

Conductivity measurements were performed at room temperature. Measurements were run in triplicates. An inoLab, Pol-Eko-Aparatura (Warsaw, Poland), conductometer was employed.

2.2.4 Precipitates and their analyses

2.2.4.1 Weight analysis

On the GP treatment of tap and mineralized waters, fine precipitates were separated from solutions by centrifugation at 500 rpm. They were collected either directly after separation or after their 3 days maintenance in aqueous suspensions at ~90°C. Weights of samples were measured in triplicates with the analytical laboratory scale RADWAG AS 220.R2 (Radom, Poland) with a precision of ±0.0001 g.

2.2.4.2 Cation chromatography, estimation of Ca^{2+}, Mg^{2+}, Na^{+} ions in solutions after the removal of deposits

Estimation of cations in solutions after the removal of deposits was performed at 22°C using ionic chromatograph 940 Professional IC Vario 1 (Metrohm, Opacz-Kolonia, Poland) with conductometric detection, 919 IC automatic sampler and Metrohm Metrosep C6 (4 × 150 mm) columns. The instrument operated involving the Metrodata 2.3 computer software. 2,2'-dipirydyne-4-carboxylic acid (PDCA) (1.7 mM) with HNO_3 (1.7 mM) served for elution. The eluent was stored in 1 L vessels pressurized at 8 p.s.i. using high-purity argon (BOC Gases, Guildford, Surrey, England, UK). The flow rate of 0.9 mL/min was maintained using a GP40 gradient pump (Dionex, Synnavale, California, USA). Injection volume was 100 µL.

2.2.4.3 Anion chromatography, estimation of SO_4^{2-}, Cl^{-} ions in solutions after the removal of deposits

Ionic chromatograph Thermo Scientific (Dionex ICS 3000) (Dionex, Synnavale, California, USA) was used. It was equipped with gradient pump, vacuum degassing system eluent generator, automatic sampler (AS-AP), AERS™300 – 2 mm suppressor, Dionex IonPac AS20 (2 × 250 mm) column with AG20 (2 × 50 mm) precolumn for ion detection and separation, respectively, and Chromeleon 7 computer software. Aqueous KOH solution (40 mM) served as an eluent. The eluent was stored in 1 L vessels pressurized at 8 p.s.i. using high-purity argon (BOC Gases, Guildford, Surrey, England, UK). The flow rate of 0.25 mL/min was maintained using a GP40 gradient pump (Dionex, Sunnyvale, California, USA). Injection volume was 10 µL. Estimations were carried out at 30°C.

2.2.4.4 Quantitative estimation of the HCO_3^{-} anion

Samples of water (100 cm^3) were titrated with 0.05 M solution of hydrochloric acid with methyl orange indicator. The HCO_3^{-} content, C, [mg/dm^3] was derived from equation (1)

$$C = \frac{V \times k \times 1000}{V_0} \quad (1)$$

where V – volume of hydrochloric acid [cm^3], k – titer of hydrochloric acid solution with respect to the HCO_3^{-} anions (3.05 mg HCO_3^{-}/cm^3) and V_0 – volume of the titrated sample [cm^3]. The measurements were run in triplicates.

2.2.4.5 Quantitative nitrogen estimation

Nitrogen content in precipitates deposited from the GP-treated ammonia added tap water was performed with CHNS Elemental Analyser (©elementar Analysensysteme GmbH, Langenselbold, Germany) on 0.1 g samples. Error of the estimation was <0.2% of the estimated value. The measurements were run in triplicates.

2.2.5 Differential scanning calorimetry (DSC)

The thermal DSC-TG-DTG analysis was carried out with the NETZSCH STA-409 simultaneous thermal analyzer (Selb, Germany) calibrated with standard indium, tin, zinc and aluminum of 99.99% purity. Samples of approximately 0.020 g deionized water and deionized water containing 3% ammonia were heated in corundum

crucibles with nonhermetic lids. Corundum (SINGLE *R) was the standard. The heating was performed under static conditions in the air in the range of 20–400°C with the 5 K min^{-1} temperature rate increase. The measurements were duplicated. They provided the ±0.5°C precision in the temperature reading.

2.2.6 Raman spectra

The spectra were taken with a Perkin-Elmer MPF44A Fluorescence Spectrophotometer (Waltham, MA, USA) equipped with a xenon lamp and 4 mL quartz cell. The spectra were recorded in the range from 350 to 650 cm^{-1} for deionized water, deionized water 0.1% ammonia added prior to and after exposure to plasma for 60 min.

2.2.7 X-ray powder diffractometry

X-ray powder diffractometer URD-6 (Cu-Kα radiation, step mode of scanning) (Freiberg, Germany) was used.

2.2.8 Diffractogram simulations

Diffractograms were taken following the paper by Shtender et al. [12]. Performed simulations were performed based on SHELX-97 software package [13] and Cambridge Structural Database [14,15].

Ethical approval: The conducted research is not related to either human or animal use.

3 Results and discussion

It was shown in our recent paper [6] that in the Raman spectrum of plain water prior to its GP treatment, a sharp peak observed around 350 nm (in Raman shift) was followed by a long weak shoulder and another sharp but less intensive peak around 700 nm. On treating that water with GP, an intensive broad peak formed at around 400 nm accompanied by a broad shoulder at around 440 nm. The intensity of the band observed around 400 nm increased with time of the GP treatment, and at the same time, the shoulder around 440 nm has transformed into a separate band. It should be underlined that these bands did not form when the water was treated without contact with the air. Based on this observation and paper by Ramya and Venkanathan [16], declusterization of the water macrostructure was postulated. The declusterization was followed by the formation of aqueous clathrates hosting molecular oxygen. These bands slowly ceased within several months of storage but immediately disappeared on contact of GP-treated water with mineral acids [6].

Raman spectra of the water treated with GP in the presence of ammonia are presented in Figure 1; one could observe the spectral pattern typical for the presence of aqueous clathrates (curves 2 and 4).

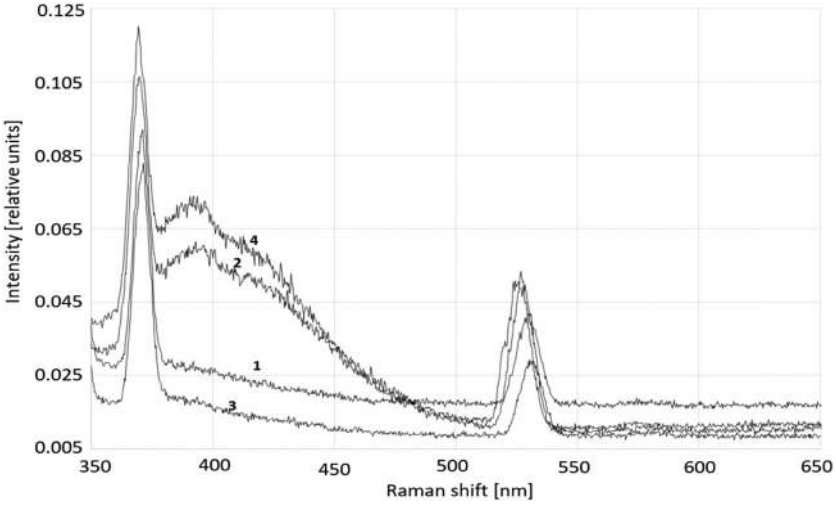

Figure 1: Raman spectra of deionized ammonia-free (1) and ammonia-containing water (3) prior to the GP treatment and these samples after such treatment, (2) and (4), respectively.

In terms of the particular peak intensities (Figure 1 and Table 1), ammonia facilitated declusterization. The GP treatment of plain, deionized and ammonia-saturated water developed the bands with shoulders at ~400 and ~430 nm, respectively. In case of plain, ammonia-free water, it was a symptom of the formation of clathrates hosting molecular oxygen. In case of water saturated with ammonia, it was an evidence of the formation of clathrates hosting ammonia. Admixture of ammonia to plain water decreased the intensity of all peaks and accompanying shoulders. Just the GP treatment of the ammonia-containing water considerably increased the intensity of all peaks.

Admixed water with either NH_3 or NaOH under study alkaline has been shown in Table 2.

Regardless of the added concentration of either NH_3 or NaOH, the pH of the nontreated deionized as well as the tap water only slightly decreased with the GP treatment time. That effect was slightly more remarkable in case of tap water. Also, that decrease in water with NH_3 was slightly more remarkable than in water alkalized with NaOH. It could suggest some evolution of ammonia as the treatment time progressed. However, the pH of the water-containing NaOH also decreased on the GP treatment. Thus, evidently, the GP treatment influenced the dissociation of the hydroxides added. Since that effect was stronger in case of ammonia, an intervention of the GP treatment into the equilibrium of the reaction

$$NH_3 + H_2O \rightleftarrows NH_4OH \rightleftarrows NH_4^+ + OH^-$$

and hydration conditions of the reaction participants could be taken under consideration. The pattern of the Raman spectra of the GP-treated water-containing ammonia (a maximum and its shoulder between 390 and 450 cm^{-1}) (Figure 1) suggests the formation of clathrates [6,16]. Nonlinear changes of pH against the GP treatment time support this assumption. The same behavior observed in case of the water treated in the air was interpreted as dependent on the treatment time changes of the structure of clathrates and the content of their interior.

The observed decrease in pH was accompanied by changes of the conductivity (Table 3). At a given concentration of the base added, these changes were irregular against the treatment time. Changes of the clathrate structure and composition on the treatment [6,16] could rationalize these irregularities.

Conductivity of the deionized water also irregularly decreased with the treatment time (Table 3). It was almost negligible in case of deionized water and remarkable in case of water-containing mineral solutes, particularly tap water. The time-depending decrease in the conductivity noted for a given kind of water was stronger in case of solutions of ammonium hydroxide than in case of solutions with sodium hydroxide. Moreover, it was slightly nonlinear against the treatment time suggesting intervention of the declusterization of the water macrostructure followed by building clusters of varying structures [6].

GP treatment of tap and highly and weakly mineralized water alkalized with either ammonia or sodium hydroxide resulted in the precipitation of a deposit. The effects became more remarkable with an increase in the content of either ammonia or sodium hydroxide added (Table 4). Ammonia provided more efficient precipitation.

On the treatment of deionized water with either ammonia or sodium hydroxide, no precipitates were formed (Table 4). Thus, apart from obvious hydrates, a possibility of the formation of aqueous clathrates including ammonia and ions, respectively, could be taken into account. DSC studies (Figure 2) carried out for deionized water containing ammonia supported such assumption.

The diagram for nontreated deionized, ammonia-free water contained several endothermic peaks

Table 1: Peak intensity in the Raman spectra of deionized water with and without ammonia prior and after GP treatment

Type of water	Peak intensity, I,[a] at wavelength [cm^{-1}]			
	365	390	410[b]	535
Plain, nontreated	0.092	0.028	0.025	0.042
Plain, GP-treated	0.105	0.059	0.053	0.052
Plain, ammonia added, nontreated	0.083	0.018	0.017	0.029
Ammonia added, GP-treated	0.120	0.072	0.060	0.050

[a] In arbitrary units. [b] A shoulder.

Table 2: pH of deionized, tap and mineralized water and its changes with the amount of either ammonia or hydroxide added and GP treatment time

NH_3/NaOH added[a] (%)	Initial pH (water free of hydroxide)	GP treatment time [min]						
		0	1	5	15	30	60	120
Deionized water[a]								
1	6.56 ± 0.05	11.12 ± 0.03	11.11 ± 0.02	11.08 ± 0.01	11.00 ± 0.03	11.02 ± 0.04	10.95 ± 0.05	10.99 ± 0.07
		12.80 ± 0.05	*12.10 ± 0.04*	*12.10 ± 0.03*	*11.98 ± 0.06*	*11.97 ± 0.02*	*11.94 ± 0.06*	*11.96 ± 0.05*
2.5		11.75 ± 0.02	11.68 ± 0.06	11.67 ± 0.03	11.52 ± 0.08	11.43 ± 0.03	11.23 ± 0.03	11.02 ± 0.02
5		11.86 ± 0.05	11.10 ± 0.07	10.52 ± 0.04	10.20 ± 0.02	10.63 ± 0.07	10.72 ± 0.03	10.34 ± 0.02
		12.06 ± 0.04	*12.03 ± 0.02*	*11.95 ± 0.06*	*11.94 ± 0.05*	*11.99 ± 0.06*	*12.01 ± 0.07*	*11.95 ± 0.08*
7.5		11.94 ± 0.04	10.53 ± 0.06	10.25 ± 0.08	10.45 ± 0.03	10.13 ± 0.08	10.56 ± 0.03	10.44 ± 0.03
10		12.10 ± 0.03	11.85 ± 0.01	11.86 ± 0.03	12.02 ± 0.07	11.93 ± 0.02	11.83 ± 0.01	11.78 ± 0.03
		12.85 ± 0.02	*12.81 ± 0.06*	*12.83 ± 0.07*	*12.87 ± 0.03*	*12.81 ± 0.01*	*12.76 ± 0.06*	*12.73 ± 0.04*
Tap water[a]								
1	7.00 ± 0.04	11.05 ± 0.02	10.95 ± 0.04	10.94 ± 0.04	10.95 ± 0.01	10.92 ± 0.03	11.02 ± 0.04	10.92 ± 0.02
		12.30 ± 0.05	*11.70 ± 0.05*	*11.65 ± 0.04*	*11.62 ± 0.05*	*11.53 ± 0.03*	*11.55 ± 0.02*	*11.53 ± 0.04*
2.5		11.46 ± 0.05	11.23 ± 0.07	11.22 ± 0.02	11.04 ± 0.06	11.06 ± 0.06	10.98 ± 0.06	10.85 ± 0.08
5		11.08 ± 0.02	11.70 ± 0.06	11.30 ± 0.04	10.80 ± 0.03	10.70 ± 0.02	10.60 ± 0.06	10.70 ± 0.03
		12.90 ± 0.05	*12.68 ± 0.03*	*12.51 ± 0.02*	*12.36 ± 0.06*	*12.28 ± 0.07*	*12.31 ± 0.06*	*12.22 ± 0.07*
7.5		11.98 ± 0.04	11.40 ± 0.06	10.62 ± 0.03	10.42 ± 0.04	10.85 ± 0.07	10.63 ± 0.03	10.32 ± 0.08
10		12.08 ± 0.03	11.56 ± 0.07	11.76 ± 0.03	11.87 ± 0.04	12.04 ± 0.02	11.93 ± 0.03	11.98 ± 0.03
		12.31 ± 0.04	*12.18 ± 0.03*	*12.11 ± 0.02*	*12.08 ± 0.06*	*12.06 ± 0.04*	*12.05 ± 0.06*	*11.97 ± 0.02*
Highly mineralized water[a]								
1	8.60 ± 0.02	10.11 ± 0.04	9.85 ± 0.06	9.82 ± 0.03	9.81 ± 0.06	8.87 ± 0.02	8.62 ± 0.06	8.31 ± 0.07
		11.42 ± 0.03	*11.40 ± 0.06*	*11.32 ± 0.03*	*11.21 ± 0.06*	*10.56 ± 0.07*	*10.41 ± 0.06*	*10.21 ± 0.04*
2.5		10.44 ± 0.04	11.11 ± 0.06	11.08 ± 0.04	11.00 ± 0.03	11.02 ± 0.02	10.95 ± 0.02	10.99 ± 0.02
5		10.82 ± 0.04	10.72 ± 0.03	10.76 ± 0.07	10.32 ± 0.03	10.24 ± 0.04	10.11 ± 0.01	10.21 ± 0.05
		11.03 ± 0.00	*10.92 ± 0.06*	*10.93 ± 0.03*	*10.74 ± 0.02*	*10.42 ± 0.07*	*10.35 ± 0.05*	*10.34 ± 0.03*
7.5		10.21 ± 0.07	9.81 ± 0.08	9.65 ± 0.04	9.62 ± 0.04	9.51 ± 0.03	9.49 ± 0.07	9.51 ± 0.02
10		11.52 ± 0.04	11.37 ± 0.06	11.32 ± 0.07	11.21 ± 0.03	11.08 ± 0.02	10.52 ± 0.01	10.21 ± 0.05
		11.03 ± 0.05	*10.95 ± 0.07*	*10.93 ± 0.03*	*10.82 ± 0.02*	*10.63 ± 0.06*	*10.18 ± 0.07*	*9.62 ± 0.03*
Weakly mineralized water[a]								
1	6.10 ± 0.03	10.11 ± 0.06	9.84 ± 0.07	9.86 ± 0.04	9.81 ± 0.02	9.62 ± 0.05	9.34 ± 0.01	9.17 ± 0.06
		12.01 ± 0.03	*11.89 ± 0.03*	*11.85 ± 0.02*	*11.62 ± 0.05*	*11.34 ± 0.04*	*10.86 ± 0.02*	*10.37 ± 0.06*
2.5		10.78 ± 0.04	11.11 ± 0.02	11.08 ± 0.04	11.00 ± 0.06	11.02 ± 0.03	10.95 ± 0.01	10.99 ± 0.04
5		11.20 ± 0.06	11.01 ± 0.07	10.65 ± 0.04	10.25 ± 0.02	10.01 ± 0.05	9.65 ± 0.06	9.51 ± 0.03
		11.92 ± 0.04	*11.93 ± 0.04*	*11.90 ± 0.02*	*10.91 ± 0.02*	*10.65 ± 0.04*	*10.53 ± 0.03*	*10.46 ± 0.06*
7.5		11.21 ± 0.04	11.01 ± 0.03	10.52 ± 0.02	10.31 ± 0.06	10.25 ± 0.02	10.12 ± 0.02	9.84 ± 0.01
10		11.43 ± 0.04	11.11 ± 0.04	11.08 ± 0.05	11.00 ± 0.06	10.02 ± 0.03	10.95 ± 0.04	10.99 ± 0.06
		11.68 ± 0.06	*11.56 ± 0.03*	*11.60 ± 0.06*	*11.51 ± 0.07*	*11.48 ± 0.03*	*11.42 ± 0.02*	*11.36 ± 0.05*

[a] Data taken in aq. NaOH solutions are given in italics.

Table 3: Conductivity of deionized, tap and mineralized water and its changes with the amount of hydroxide added and the GP treatment time

NH_3/NaOH added[a] [%]	Water	GP treatment time [min]						
		0	1	5	15	30	60	120
Deionized water								
1	0.001 ± 0.001	0.326 ± 0.004	0.354 ± 0.002	0.364 ± 0.002	0.353 ± 0.001	0.342 ± 0.005	0.352 ± 0.005	0.322 ± 0.002
		0.392 ± 0.005	*0.393 ± 0.004*	*0.395 ± 0.002*	*0.396 ± 0.002*	*0.397 ± 0.002*	*0.394 ± 0.001*	*0.392 ± 0.002*
2.5		0.455 ± 0.006	0.353 ± 0.003	0.315 ± 0.002	0.327 ± 0.002	0.328 ± 0.005	0.294 ± 0.006	0.313 ± 0.003
5		0.355 ± 0.003	0.367 ± 0.005	0.349 ± 0.002	0.310 ± 0.004	0.305 ± 0.006	0.323 ± 0.003	0.302 ± 0.005
		0.415 ± 0.001	*0.407 ± 0.006*	*0.409 ± 0.005*	*0.397 ± 0.001*	*0.403 ± 0.002*	*0.391 ± 0.003*	*0.394 ± 0.002*
7.5		0.352 ± 0.007	0.315 ± 0.005	0.328 ± 0.004	0.303 ± 0.007	0.297 ± 0.004	0.315 ± 0.002	0.323 ± 0.005
10	0.006 ± 0.002	0.912 ± 0.003	0.862 ± 0.002	0.916 ± 0.003	0.954 ± 0.002	0.967 ± 0.003	0.995 ± 0.003	1.013 ± 0.002
		0.455 ± 0.003	*0.444 ± 0.003*	*0.446 ± 0.001*	*0.439 ± 0.006*	*0.436 ± 0.002*	*0.435 ± 0.005*	*0.424 ± 0.004*
Tap water								
1	0.844 ± 0.002	0.959 ± 0.004	0.756 ± 0.009	0.794 ± 0.005	0.813 ± 0.002	0.622 ± 0.004	0.564 ± 0.002	0.388 ± 0.007
		0.953 ± 0.004	*0.904 ± 0.005*	*0.874 ± 0.003*	*0.866 ± 0.002*	*0.866 ± 0.005*	*0.815 ± 0.001*	*0.792 ± 0.003*
2.5		1.107 ± 0.003	0.820 ± 0.006	0.625 ± 0.002	0.513 ± 0.005	0.347 ± 0.006	0.285 ± 0.002	0.025 ± 0.001
5		1.127 ± 0.006	0.953 ± 0.002	0.842 ± 0.003	0.637 ± 0.005	0.529 ± 0.007	0.356 ± 0.003	0.205 ± 0.001
		1.132 ± 0.005	*1.124 ± 0.002*	*1.116 ± 0.002*	*0.993 ± 0.003*	*0.902 ± 0.004*	*0.697 ± 0.001*	*0.563 ± 0.002*
7.5		1.237 ± 0.003	1.028 ± 0.006	0.814 ± 0.002	0.653 ± 0.002	0.356 ± 0.006	0.267 ± 0.004	0.118 ± 0.006
10		1.184 ± 0.008	0.425 ± 0.002	0.316 ± 0.004	0.307 ± 0.003	0.319 ± 0.002	0.304 ± 0.002	0.302 ± 0.001
		1.224 ± 0.002	*1.193 ± 0.008*	*1.195 ± 0.006*	*1.027 ± 0.003*	*0.938 ± 0.004*	*0.815 ± 0.003*	*0.635 ± 0.004*
Highly mineralized water								
1	0.115 ± 0.004	0.213 ± 0.005	0.235 ± 0.003	0.249 ± 0.06	0.247 ± 0.003	0.238 ± 0.006	0.176 ± 0.007	0.164 ± 0.004
		0.426 ± 0.003	*0.418 ± 0.004*	*0.364 ± 0.001*	*0.352 ± 0.002*	*0.324 ± 0.005*	*0.306 ± 0.002*	*0.268 ± 0.003*
2.5		0.325 ± 0.006	0.317 ± 0.004	0.300 ± 0.002	0.294 ± 0.002	0.273 ± 0.005	0.263 ± 0.003	0.253 ± 0.002
5		0.414 ± 0.003	0.357 ± 0.003	0.315 ± 0.004	0.244 ± 0.003	0.239 ± 0.001	0.185 ± 0.002	0.155 ± 0.003
		0.414 ± 0.009	*0.383 ± 0.009*	*0.393 ± 0.003*	*0.373 ± 0.004*	*0.367 ± 0.002*	*0.295 ± 0.003*	*0.263 ± 0.002*
7.5		0.328 ± 0.006	0.353 ± 0.003	0.363 ± 0.005	0.353 ± 0.006	0.348 ± 0.003	0.354 ± 0.002	0.324 ± 0.003
10		0.985 ± 0.003	0.428 ± 0.007	0.419 ± 0.004	0.403 ± 0.006	0.362 ± 0.003	0.352 ± 0.002	0.322 ± 0.001
		0.526 ± 0.002	*0.498 ± 0.005*	*0.489 ± 0.001*	*0.464 ± 0.004*	*0.413 ± 0.002*	*0.366 ± 0.002*	*0.316 ± 0.005*
Weakly mineralized water								
1	0.054 ± 0.002	0.387 ± 0.004	0.329 ± 0.003	0.284 ± 0.002	0.283 ± 0.005	0.241 ± 0.001	0.198 ± 0.005	0.182 ± 0.002
		0.353 ± 0.002	*0.355 ± 0.003*	*0.336 ± 0.003*	*0.308 ± 0.005*	*0.269 ± 0.002*	*0.214 ± 0.004*	*0.193 ± 0.002*
2.5		0.254 ± 0.006	0.236 ± 0.007	0.210 ± 0.003	0.179 ± 0.003	0.163 ± 0.002	0.159 ± 0.003	0.152 ± 0.003
5		0.397 ± 0.006	0.350 ± 0.002	0.310 ± 0.003	0.286 ± 0.001	0.243 ± 0.002	0.201 ± 0.005	0.165 ± 0.002
		0.397 ± 0.002	*0.399 ± 0.003*	*0.370 ± 0.003*	*0.363 ± 0.003*	*0.326 ± 0.002*	*0.296 ± 0.005*	*0.236 ± 0.004*
7.5		0.484 ± 0.005	0.432 ± 0.007	0.372 ± 0.002	0.326 ± 0.002	0.279 ± 0.003	0.213 ± 0.001	0.182 ± 0.002
10		0.536 ± 0.008	0.418 ± 0.003	0.400 ± 0.006	0.364 ± 0.003	0.322 ± 0.002	0.282 ± 0.007	0.236 ± 0.004
		0.417 ± 0.002	*0.419 ± 0.003*	*0.395 ± 0.003*	*0.384 ± 0.004*	*0.354 ± 0/005*	*0.347 ± 0.002*	*0.315 ± 0.002*

[a] Data taken in aq. NaOH solutions are given in italics.

Table 4: Amount [mg] of precipitation after 120 min GP treatment

Type of water	Additive [%]					
	NaOH			NH_3		
	1	5	10	1	5	10
Deionized	0	0	0	0	0	0
Tape	98	112	118	136	152	153
Highly mineralized	112	123	148	158	173	182
Weakly mineralized	46	42	43	79	75	76

associated with the rearrangements of the water macrostructure. These effects were exhaustively discussed by Prouzet et al. [17]. The pattern of the curve for deionized, nontreated water containing 3% ammonia was entirely different. Initially, it strongly rose as a result of an endothermic process. Then, around 60°C, the curve became almost planar. Two slightly endothermic effects at 88.4 and 131.5°C could be recognized on that segment which relatively slightly elevated up to 150°C. The course of that segment pointed to an overall endothermic character of the changes occurring in the sample macrostructure. After the 1- and 5-min treatment, the pattern of the curve remained identical; however, the overall process turned into less endothermic. The decrease in the endothermic character of the overall process (line 1 in Figure 2) followed an increase in the treatment time of the samples. Likely, the endothermic process was associated with declusterizing of the water macrostructure on the GP treatment. That process was evidently facilitated by ammonia.

In the sample of the ammonia-containing water treated for 30 min, the deal of the declusterization process was significantly reduced. In contrast to former curves, the semi-planar section of that line declined up to about 145°C in order to increase again above that temperature. The endothermic effect formerly observed between 88 and 90°C appeared at 89.7°C. It was essentially stronger, whereas the effect formerly observed between 131.5 and 127.9°C appeared at 123.2°C and was hardly recognizable. These differences evoked by the treatment pointed to a possibility of the formation of aqueous ammonia clathrates.

Data in Table 5 demonstrate efficiency of the removal of ions responsible for the water hardness increasing with the concentration of ammonia added and the GP treatment time. Accompanying demineralization of water in terms of the removal of sodium and chloride ions was negligible, and a higher concentration of ammonia added obstructed, to a certain extent, the removal of those ions.

It was interesting that precipitates formed on the treatment from each water-containing mineral did not exhibit any tendency to turn into a scale. Such behavior could result from ligation of the Ca and Mg atoms with the NH_3 ligands.

Alkaline earth atoms readily coordinate O-ligands and that ability can be controlled by their counterions [18]. These central atoms can also coordinate N-ligands. For instance, there are known numerous coordination compounds of magnesium and calcium with pyridine ligands [19]. These central atoms coordinate four and six

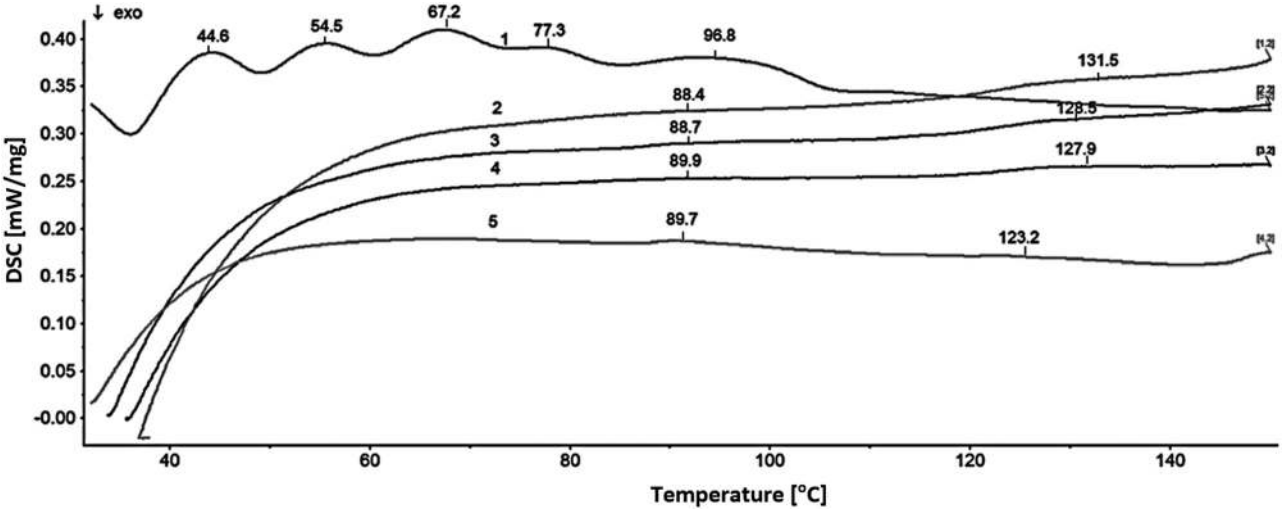

Figure 2: Differential scanning calorimetry (DSC) diagrams for nontreated deionized water (1), deionized nontreated water with 3% ammonia (2), deionized water with 5% ammonia treated for 1 (3), 5 (4) and 30 min (5).

Table 5: Amount of ions [mg/L] remaining in the treated water containing 0.5 and 10% ammonia after separation of precipitate

Type of water	GP treatment duration [min]					
	0	1	15	30	60	120
	Ion content [mg/L]					
Ca^{2+}						
Deionized	0.25	0.1	0.05	0.03	0.03	0.02
Tape[a]	193.27	185.2	180.3	176.3	175.5	174.3
		73.2	*20.4*	*12.3*	*10.2*	*6.5*
Highly mineralized	368.92	125.8	53.84	12.32	10.85	8.21
Weakly mineralized	44.9	11.5	10.2	9.52	5.23	4.25
Mg^{2+}						
Deionized	0.12	0.11	0.05	0.04	0.04	0.03
Tape[a]	46.21	45.8	43.2	40.9	39.8	38.9
		38.4	*32.14*	*25.63*	*12.39*	*5.32*
Highly mineralized	73.209	68.72	65.23	53.28	31.02	17.21
Weakly mineralized	17.01	15.07	10.25	6.52	4.25	2.18
Na^{+}						
Deionized	0.08	0.07	0.08	0.08	0.06	0.07
Tape[a]	23.18	22.1	21.9	21.7	21.6	21.5
		22.8	*22.5*	*22.4*	*22.38*	*22.18*
Highly mineralized	54.71	53.8	53.4	53.5	53.2	53.2
Weakly mineralized	1	0.95	0.95	0.94	0.94	0.93
HCO_3^{-}						
Deionized	18.3	13.5	8.98	7.65	6.21	5.14
Tape[a]	351.9	346.8	345.8	344.7	344.6	344.2
		128.7	*83.5*	*35.8*	*34.8*	*33.2*
Highly mineralized	1721.9	438.2	211.5	193.4	128.3	67.2
Weakly mineralized	186.7	56.8	36.8	23.5	14.9	12.3
$SO_4^{=}$						
Deionized	1.28	0.98	0.87	0.69	0.62	0.43
Tape[a]	51.2	50.9	50.8	50.1	49.9	49.8
		34.8	*16.8*	*12.8*	*8.7*	*6.2*
Highly mineralized	40.5	30.1	23.1	18.9	14.3	9.1
Weakly mineralized	43.62	29.5	25.3	20.2	14	10.8
Cl^{-}						
Deionized	0.01	0.01	0.01	0	0.01	0.01
Tape[a]	6.52	6.48	6.42	6.39	6.38	6.38
		6.32	*6.25*	*6.08*	*6.05*	*6.07*
Highly mineralized	7.8	7.68	7.65	7.52	7.52	7.46
Weakly mineralized	3.19	3.15	3.11	3.11	3.09	3.02

[a]The upper values are for the treatment of 0.5% ammonia added and the lower values in italics are for the treatment water with 10% ammonia.

NH_3 molecules. The smaller Mg atom is a stronger electron donor than the Ca atom. The structure of the first solvation shell is sharper for Mg, which has a larger charge and smaller radius than Ca. Weak solvation leads to rapid dynamics in terms of the diffusion coefficients of the NH_3 molecules [20,21]. Thus, likely, Mg and Ca carbonates and sulfates could coordinate NH_3 ligands.

Indeed, the formula of the deposition immediately after its precipitation, $Ca_{0.85}Mg_{0.10}Fe_{0.05}[CO_3](NH_3)_2$, and after being suspended for 3 days in the solution, turned into $Ca_{0.83}Mg_{0.12}Fe_{0.05}[CO_3](NH_3)_2$, pointing to a gradual passing of calcium into the solution. It might suggest that, for instance, ionic interactions could contribute to the formation of precipitates.

The rhombohedral crystals of the precipitate belonged to the $R\bar{3}c(167)$ space group. Relevant network constants and atom coordinates are given in Table 6.

Experimental and numerically simulated diffractograms of freshly deposited precipitates are presented in Figures 3 and 4, respectively. Their patterns and localization of particular reflexes satisfactorily fitted one another.

After three days in suspension at around 90°C, the crystallographic structure of the precipitate slightly changed (Table 7 and Figures 5, 6). The volume of the crystallographic cell remained unchanged. The shift of the diffraction reflexes toward higher 2θ angles (Figure 7) informed on decrease in the network constants due to decrease in the calcium content and, simultaneously, an increase in the magnesium content.

The presented study proposes the removal of permanent and temporary water hardness at room temperature and without any necessity of the removal of deposit which was formed. For this purpose, water should be blended with ammonia followed by the treatment with GP. Admixture of ammonia makes water noncorrosive. The stabilization of the rhombohedral precipitate against scaling is afforded by coordination of ammonia ligands to the Mg and Ca atoms.

Thus, the treated water was suitable for protecting water-heating systems and water-transmitting pipelines against the scale and corrosion, eliminating other chemical, physical and physicochemical methods used for that purpose.

Additionally, on the GP treatment of ammonia-containing water, the formation of aqueous clathrates of ammonia was postulated. Water with ammonia within clathrates may serve as an alternative, environmentally benign nitrogen fertilizer. Resulting precipitates can also be utilized for the same purpose.

Table 6: Network constants and atom coordinates of the atoms of freshly precipitated deposit

Network constants		**a = 0.4985 nm, c = 1.6994 nm, V = 0.3646 nm^3** [a]			
Atom coordinates	Elements	Crystallographic axis	x	y	z
	O	18e	0.2577	0	1/4
	0.85Ca + 0.10Mg + 0.05Fe	6b	0	0	0
	C	6a	0	0	1/4

[a] The volume of the crystallographic cell.

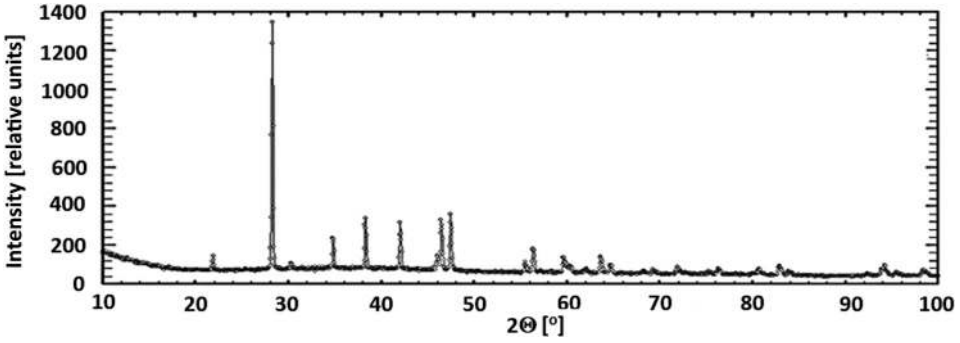

Figure 3: Experimental diffractogram of freshly deposited precipitate.

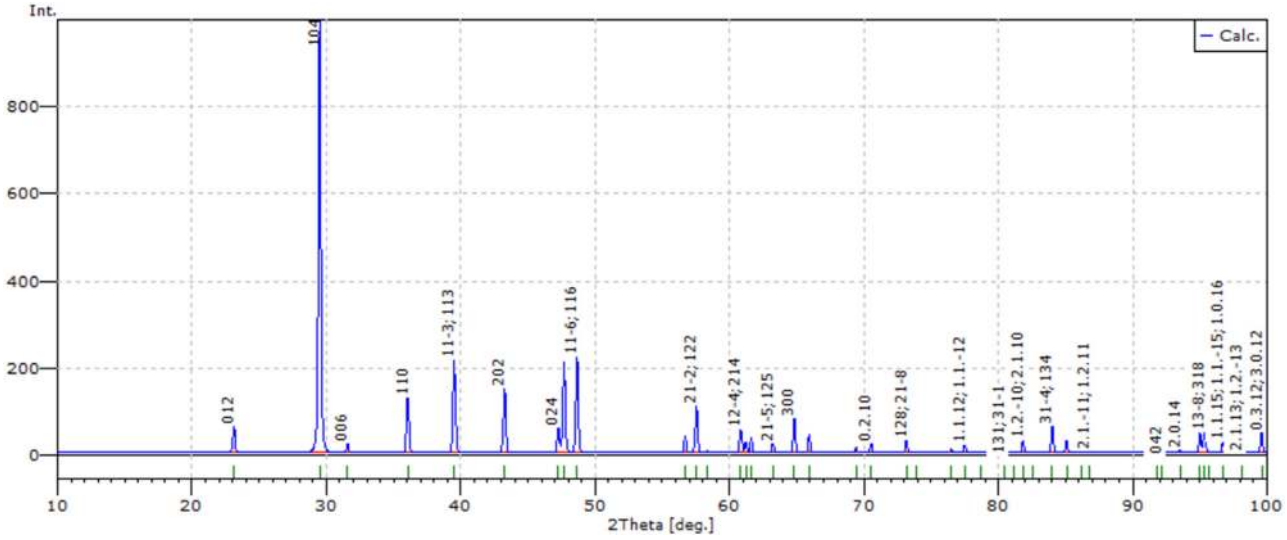

Figure 4: Numerically simulated diffractogram of freshly deposited precipitate.

Table 7: Network constants and atom coordinates of the atoms of precipitated deposit taken after 3 days

Network constants		**a = 0.4979 nm, c = 1.6989 nm, V = 0.3646 nm^3** [a]			
Atom coordinates	Elements	Crystallographic axis	x	y	z
	O	18e	0.2577	0	1/4
	0.83Ca + 0.12Mg + 0.05Fe	6b	0	0	0
	C	6a	0	0	1/4

[a] The volume of the crystallographic cell.

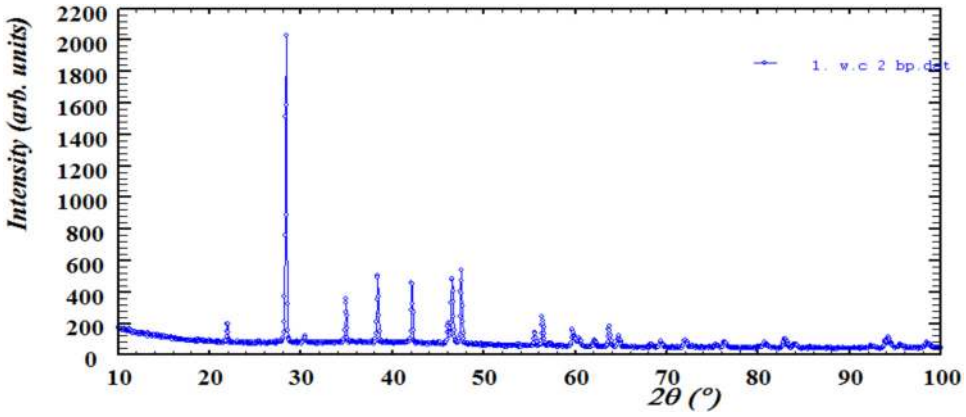

Figure 5: Experimental diffractogram of deposited precipitate stored for 3 days.

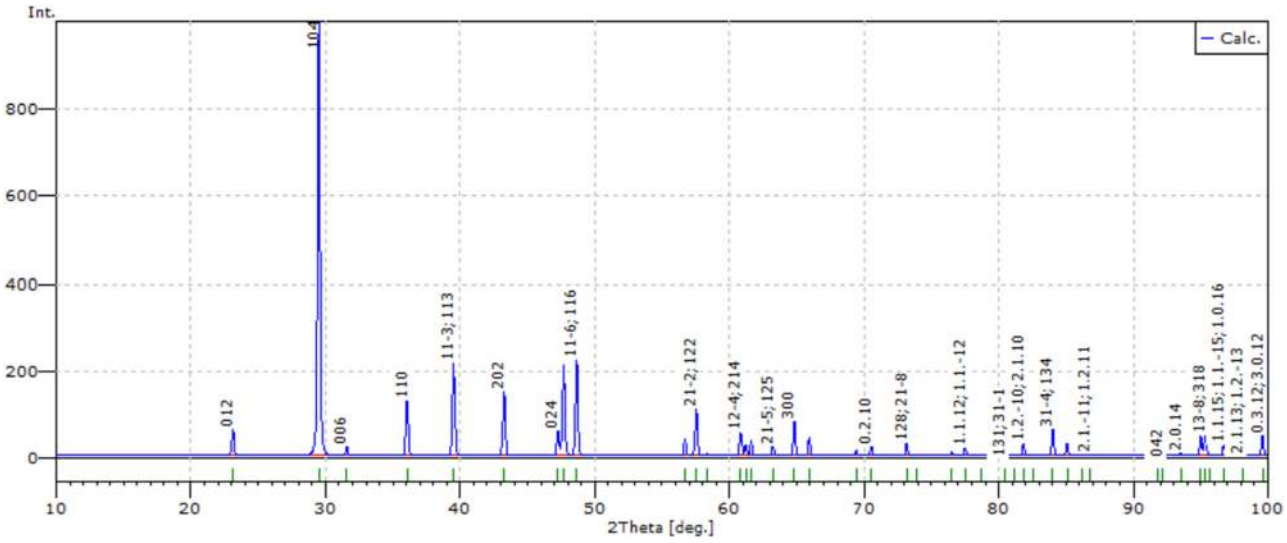

Figure 6: Numerically simulated diffractogram of deposited precipitate stored for 3 days.

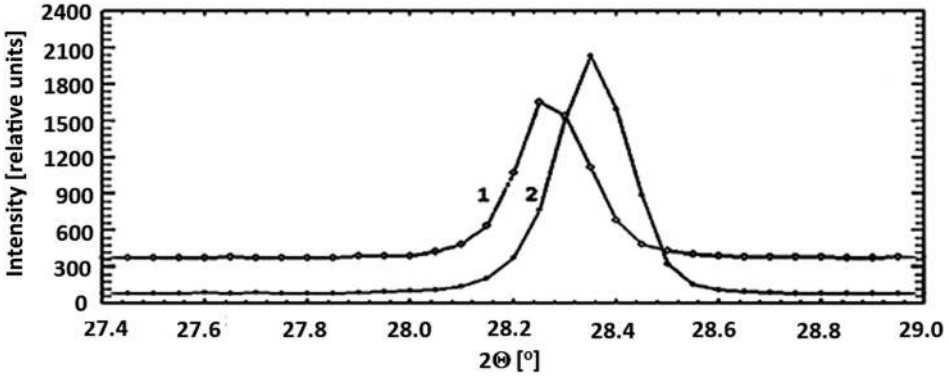

Figure 7: The shift of reflexes in the diffractograms of precipitates due to decrease in the calcium content and simultaneously increase in the magnesium content; (1) and (2) diffractograms of freshly deposited and collected after 3-days precipitates, respectively.

4 Conclusions

1. Permanent and temporary water hardness-removed water at room temperature to which ammonia was admixed is subjected to treatment with low-pressure, low-temperature GP of low frequency.
2. Fine deposit which is formed does not turn into scale even within 3-day maintenance at about 90°C.
3. Water treated under ammonia with low-pressure, low-temperature GP of low frequency protects water-heating systems and water-transmitting pipelines against scale and corrosion providing elimination of other chemical, physical and physicochemical methods used for that purpose.
4. Water treated under ammonia with low-pressure, low-temperature GP of low frequency as well as precipitates can serve as an alternative, environmentally benign nitrogen fertilizer.

Conflict of interest: The authors declare no conflict of interest.

References

[1] Chaplin M, Water www.1.lsbu.ac.uk/water/water_descaling.html [cited Oct. 22nd 2018].
[2] Crabtree M, Eslinger D, Fletcher P, Johnson A, King G. Fighting scale-removal and prevention. Oilfield Reviev. 1999;Autumn:30–48.
[3] Nitsch C, Heitland H-J, Marsen M, Schluessler H-J. Cleansing agents. Ullman's Encyclopedia of Industrial Chemistry. Weinheim: Wiley–VCH; 2005.
[4] Weingaertner H. Water. In: Ullman's Encyclopedia of Industrial Chemistry. Weinheim: Wiley–VCH; 2006.
[5] Kamal MS, Hussein I, Mahmoud M, Sultan AS, Saad MAS. Oilfield scale formation and chemical removal: a review. J Petr Sci Eng. 2018;171:127–39.
[6] Bialopiotrowicz T, Ciesielski W, Domanski J, Doskocz M, Fiedorowicz M, Graz K, et al. Structure and physicochemical properties of water treated with low-temperature low-frequency glow plasma. Curr Phys Chem. 2016;6:312–20.
[7] Chwastowski J, Ciesielska K, Ciesielski W, Khachatryan K, Kołoczek H, Kulawik D, et al. Structure and physicochemical properties of water treated under nitrogen with low-temperature glow plasma. Water. 2020;12:1314. doi: 103390/w12051314.
[8] Ciesielska A, Ciesielski W, Khachatryan K, Koloczek H, Kulawik D, Oszczeda Z, et al. Structure and physicochemical properties of water treated under methane with low-temperature glow plasma of low frequency. Water. 2020;12:1638. doi: 10.3390/w12061638.
[9] Ciesielska A, Ciesielski W, Khachatryan K, Koloczek H, Kulawik D, Oszczeda Z, et al. Structure and physicochemical properties of water treated under carbon dioxide with low-temperature low-pressure glow plasma of low frequency. Water. 2020;12:1920. doi: 10.3390/w12071920.
[10] Chwastowski J, Ciesielski W, Khachatryan K, Kołoczek H, Kulawik D, Oszczęda Z, et al. Water of increased content of molecular oxygen. Water. 2020;12:2488. doi: 10.3390/w12092488.
[11] Reszke E, Yelkin I, Oszczęda Z. 2017. Plasming lamp with power supply. Polish Patent 2017, PL 227530 B1.
[12] Shtender VV, Pavlyuk VV, Zelinska OYa, Nitek W, Paul-Boncour V, Dmytriv GS, et al. The Y–Mg–Co ternary system: alloys synthesis, phase diagram at 500°C and crystal structure of the new compounds. J Alloys Compd. 2019;812:152072. doi: 10.1016/j.jallcom.2019.152072.
[13] Sheldrick GM. SHELXS-97and SHELXL-97 – WinGX Version. Release 97–2. Germany: University of Göttingen; 1997.
[14] Rodriguez-Carvajal J. Recent advances in magnetic structure determination by neutron powder diffraction. Phys B. 1993;192:55–69.
[15] Roisnel T, Rodriguez-Carvajal J. WinPLOTR, a windows tool for powder diffraction pattern analysis. Mater Sci Forum. 2001;378–381:118–23.
[16] Ramya KR, Venkathnathan A. Density functional theory study of oxygen clathrate hydrates. Indian J Chem. 2013;52A:1063–5.
[17] Prouzet E, Brubach J-B, Roy P. Differential scanning calorimetry study of the structure of water confined within AOT lamellar mesophases. J Phys Chem B. 2010;114:8081–8.
[18] Chaban VV, Prezhdo OV. Electron solvation in liquid ammonia: lithium, sodium, magnesium, and calcium as electron sources. J Phys Chem B. 2016;120:2500–6.
[19] Chaban VV, Andreeva NA, Vorontsov-Velyaminova PN. A weakly coordinating anion substantially enhances carbon dioxide fixation by calcium and barium salts. Energy Fuels. 2017;31:9668–74.
[20] Tomasik P, Ratajewicz Z. Pyridine–metal complexes. In: Newkome GR, Strekowski L, editors. Interscience. Vol. 1, ch. 2, New York: J. Wiley; 1985.
[21] Kaufman Katz A, Glusker JS, Beebe SA, Bock CW. Calcium ion coordination: a comparison with that of beryllium, magnesium, and zinc. J Am Chem Soc. 1996;118:5752–63.